

Comparison of Effectiveness of Repair Systems between RC Beams Repaired with Sprayed Fiber Reinforced Polymer and Fiber Reinforced Mortar

H. K. Lee^{a,*}, W. C. Seaman^{a,b}

^a Department of Civil, Architectural, and Environmental Engineering,
University of Miami, Coral Gables, FL 33124-0620

^b PBS&J Inc., 2001 NW 107th Ave., Miami, FL 33172

Abstract

This paper presents the result of an experimental study conducted to investigate the effectiveness of sprayed fiber reinforced polymer (SFRP) and fiber reinforced mortar (FRM) as repair materials for damaged concrete beams. The objective of this investigation was to gain a better understanding of the material characteristics of SFRP and quantify its repair abilities by comparing and contrasting it to FRM. A series of three-point bending tests were conducted on precracked reinforced concrete (RC) beams repaired with SFRP and FRM to quantify the repair abilities of these two repair systems. The tests yielded complete load-deflection curves from which the increase in load-capacity, ductility and energy absorption was evaluated. The data from these tests as well as the testing observations were interpreted to establish an understanding of the material characteristics and how they interact with the concrete beam to repair it. The results show that SFRP is a viable alternative for use as a repair system for concrete.

Keywords: Fiber reinforced mortar (FRM), Sprayed fiber reinforced composites (SFRP), Repair systems, Load capacity and ductility, Precracked RC beams

Cement & Concrete Composites, submitted for possible publication.

* Corresponding author. Tel: (305) 284-3457; e-mail: hlee@miami.edu

1. Introduction

With the continued deterioration of existing concrete structures, the need for an effective repair system is becoming increasingly important. While there are numerous concrete repair systems available, a system that is quick and simple to apply, effective in repairing and strengthening the damaged concrete, and cost effective is still unavailable. In applications such as highway bridges, where closure of the roadways above and below could have huge economic impacts, the repair system must be installed in-situ, quickly, and then must set up and become effective within a short amount of time. Given the huge expense of replacing the bridge, the system must also last long enough to offset the replacement costs.

A new method for repairing concrete has emerged as the possible solution to all of these needs. Sprayed fiber reinforced polymers (SFRP) have been in use for several years, however their use as a repair material for concrete is relatively new. The polymer materials offer some distinct advantages over cement-based repair materials. Polymer materials have a high tensile strength, easily exceeding that of concrete; high bond strength, decreasing the probability of a sudden debonding failure; can be sprayed onto the repair surface, greatly simplifying and speeding up the installation process; and cure in a matter of hours, minimizing the amount of time required for the repair. As with any material, there are always disadvantages to counter the advantages, however with polymer materials the key disadvantage is a lack of data (Tang and Podolny, 1998). There are currently less than a hundred bridge projects currently employing polymer materials in the world (Ref. 10), and of those at least a third of them have been built since 1996. This lack of long term data combined with the lack of design experience has greatly hindered the development and progress of polymer materials as a viable alternative for concrete repair and rehabilitation.

Given the extremely advanced nature and the relatively unknown characteristics of the polymer materials, a simple and universally known material needs to be chosen as a basis for comparison. Fiber reinforced mortar (FRM) is commercially available, commonly used, and very simple in application and characteristics. Given the relatively low tensile strength of mortar (Issa and Shafiq, 1999), any additional tensile strength seen in the beam repaired with FRM can be attributed directly to the fiber reinforcing in the mortar mix. Also, mortar has been a common building material for hundreds of years, translating into an abundance of available research, testing, and data on its characteristics.

Of the research papers available within the past fifteen years, the majority of them focus on a specific material characteristic of FRM, rather than its use as a concrete repair system. However, the material characteristics being investigated can be directly correlated to the use of FRM as a concrete repair system. In research performed by Issa and Shafiq (1999), the effect of fiber spacing and fiber size on the fatigue crack growth characteristics and corresponding toughness strength are explored. Their data concluded no discernable link between the two for crack growth, but fracture toughness was increased with decreased fiber spacing. Glinicki (1994) performed research on the toughness of steel fiber reinforced mortar by varying the loading rate on the specimen. He also varied the fiber content in the specimens, finding that the fracture toughness generally increased with increased fiber content. The effects of different types of fibers were explored by Wang et al. (1990). They tested specimens with aramid, high-strength high-modulus polyethylene, and polypropylene fibers at volume fractions less than three percent and reported tensile properties of each. Zhu and Chung (1997) used carbon fibers in a mortar mix to decrease the shrinkage during drying. Adding five percent of the cement weight in carbon fibers produced a fifty percent decrease in shrinkage of the specimen at twenty-four hours. This decrease in shrinkage resulted in increased bond strengths whereby the brick to mortar bond strength tested increased by 150% for tension and 110% for shear.

There are several papers that exploit the simple characteristics of FRM, using the mortar as a medium to test the effects of a different material. Soroushian et al. (1991) used FRM as the medium to research the effects of latex additives in the mix. While they found that the latex did not significantly affect the flexural strength of the fiber-reinforced mortar, it did improve the flexural toughness and decrease the permeability. Fu and Chung (1997) used carbon fibers in a mortar mix as conducting fibers for an electrical current. This electrical current was used to monitor the specimen without sensors, creating a "self-monitoring" specimen. The primary purpose of the paper was to examine the effects of curing age on the conductivity of the fibers.

The study presented herein investigates the effectiveness of SFRP and FRM as repair materials for damaged concrete beams. The objective of this investigation is to gain a better understanding of the material characteristics of SFRP and quantify its repair abilities by comparing and contrasting it to FRM. To quantify the repair abilities of these two systems, precracked concrete beams were repaired with them and then tested to failure. The data

from these tests as well as the testing observations will then be interpreted to establish an understanding of the material characteristics and how they interact with the concrete beam as a repair material.

2. Testing Methodology

The testing method utilized for this research is based upon the “Standard Test Method for Determining Fracture Properties of Concrete”, Draft 10, September 26, 2001, prepared by ACI 446 task group (Ref. 12). This method was chosen because it isolates the loading to the tension face of the specimen. This concentration of force accentuates the fracture strength of the specimen. When the repair material is applied to the tension face of the cracked specimen, the loading is concentrated on the repair material. This allows data to be gathered which can help to understand if the repair system is truly beneficial and thereby gain an understanding of how the repair material is benefiting the cracked specimen.

3. Specimen

The test method utilized 100 x 100 x 450 mm concrete specimens. The specimens were all prepared in a mold made of 19 mm (3/4”) plywood. Each wood mold cast sixteen specimens in a 4 x 4 arrangement, allowing for easy transportation and demolding. The wood molds were constructed, painted with a waterproofing sealant, and then wiped down with oil to facilitate demolding. A #2 smooth rebar was then suspended in each specimen at 50 mm (2”) clear from the bottom of the mold. All specimens were cast at the same time and then covered overnight. After 24 hours of curing, the specimen were demolded and placed in a humidity-controlled room to complete the curing process.

Prior to coating the specimens with the repair material, all specimens were loaded to induce an initial crack. Since the specimens were minimally reinforced, the load required to create a crack associated with the ultimate load was calculated and set as the maximum load for pre-cracking. The specimen was then placed in the MTS loading machine and loaded at a rate of 0.375 mm/sec to create this initial crack. The crack was determined both visually on the specimen and by monitoring the loading curve for a sudden drop in load. These peak loads were recorded for comparison with the peak load of the repaired specimens.

The specimens that would be coated with the SFRP were removed from the humidity room after 31 days and the polymer was applied. Application of the polymer was a multi-step procedure. First, the specimens were prepared for application by sandblasting the face of the beam to receive the polymer. This was done to clean and roughen the application face, allowing for a higher quality bond. Simultaneously, the epoxy resin was preheated so that it would be at a desired viscosity for spraying. The polymer was applied in three layers. Because the combination of the fibers and the epoxy resin would be too viscous to spray through a gun, the epoxy resin and the fibers were sprayed separately. When spraying begins, the two liquids were drawn into a manifold and mixed, then pumped into the supply line of the spray gun.

An initial thin layer without fibers is sprayed through a standard spray gun (Figure 1 (a)). This layer acts as a base for the remaining layers, creating a consistent bond with the specimen and completely coating the application face. Any large cracks on the application surface can be filled during spraying of this layer. The fibers are sprayed on next through a pneumatic powered chopping spray gun (Figure 1 (b)). This gun consists of a rotary chopper with blades placed radially. With all blades installed, the fiber length is 13 mm; with every other blade removed, the fiber length is 26 mm and so on. For this research, the fibers were applied at 13 mm length and fifteen percent by volume. There are two rubber wheels that spin and pull the fiber through the gun. The fibers used in this study were a multi-filament E-glass strand roving. The epoxy resin is provided as two separate liquids, the epoxy resin and a catalyst. All available engineering data for the epoxy resin and the E-glass fibers can be taken from Lee et al. (2003). After application of the fibers, the epoxy resin is sprayed on to completely coat the fibers (Figure 1 (c)). The final thickness of the layer was measured to be 3.2 mm. Once coated, the repaired specimens were left to set for a minimum of two weeks.

The specimens that would be coated with FRM were removed from the humidity room after 105 days and the mortar was applied. Application of the FRM was relatively simple compared to the SFRP. A fifty pound premixed sack of surface bonding cement was used (Figure 2). The premixed cement contains the fibers, Type I Portland cement, lime, sand, and special additives. The volume fraction of the fibers was measured to be roughly 5% (Figure 3). Exact amounts of each ingredient and types of fibers cannot be reported as they are considered proprietary. First, the specimens were prepared for application by wiping

them down with a damp cloth to remove any excess material and dampen the application surface. Twenty pounds of the premixed cement was mixed with two liters of water in a bucket. Using a standard mixing stick, the cement and water were mixed for ten minutes to make the mortar (Figure 4). Using a trowel, the wet mortar was then applied to each specimen. The mortar was applied to a one quarter inch thickness (Figure 5), and then the specimens were placed back into the humidity room for proper curing. All specimens were tested 108 days after casting.

4. Testing Apparatus

Two spherically shaped blocks with an outside diameter of 50 mm (2") support the specimen. One support block is supported on a rod of the same length as the block (Figure 6 (a)); the other support block is supported on a ball of 9.5 mm (3/8") diameter at its midpoint (Figure 6 (b)). The load is applied with a spherically shaped loading block with an outside diameter of 50 mm (2"). The load is applied at the midpoint for the beam. A rubber bearing pad of 3.2 mm (1/8") thickness is used at each block to ensure even loading along the contact surface.

The yoke shown in Figure 10 is used to measure the deflection at the midpoint of the specimen. The yoke is made of 3.2 mm (1/8") thick aluminum that has two threaded holes at one end and two slotted clearance holes at the other end. At the midpoint of the long span, there are legs that extend up from the main body of the yoke and support a bridge piece. The bridge piece is interchangeable and supports the linear variable differential transformer (LVDT), which measures the deflection at the midspan of the beam relative to the neutral axis. The second support piece for the yoke is a c-shape with threaded holes at the end of each leg. To connect the yoke to the specimen, pointed bolts are used in the threaded holes to contact the specimen at its neutral axis. The bolts should be directly over the support blocks of the loading apparatus. The bridge is then installed and the LVDT is adjusted to zero.

5. Testing Procedure

Once the yoke is attached to the specimen, the specimen is placed on the loading block and then the ram is moved up until the specimen comes into contact with the support blocks (Figure 8). The specimen is then logged into the computer, the computer displacement and load are set to zero, and the test is started. The test loading rate is 0.015 mm/second, with a maximum load of 45 kN. The deflections are manually recorded every 5 seconds until the specimen reaches failure. Failure was determined by monitoring the load to displacement curve and watching for the major drop in load. In addition, the specimen was visually monitored for cracks.

6. Test Results

The specimens repaired with SFRP exhibited a sharp drop in the resisted load at the moment of cracking. This drop in load was normally accompanied by a loud sound, signifying the failure of the polymer. This is illustrated in Figure 9 and the test results for all SFRP specimens are listed in Table 1.

The moment of failure was harder to pinpoint for the FRM specimens. Because of the low tensile strength of mortar, there was no loud sound to associate with its failure. The bond between the mortar and fiber reinforcing was strong enough that the fiber reinforcing engaged as soon as the mortar was stressed, so there was no sharp drop in the resisted load. As a result, failure of the FRM specimens was determined to be the point when the slope of the loading to displacement curve started to level off. This is illustrated in Figure 10 and the test results of this testing are listed in Table 2. The comparison of load-displacement curves between specimens repaired with SFRP and FRM is shown in Figure 11.

For all specimens, the energy absorbed by the specimen prior to failure was calculated by taking the area under the loading curve. This area was calculated using Simpson's integration method in conjunction with MATLAB. This failure energy is used later in the paper to quantify the ductility of the materials.

7. Discussion of Results

The purpose of this research was to compare the effectiveness of two different types of concrete repair systems. In order to clearly layout what has been learned through this research, this discussion will cover each repair system independently and then compare the two systems to one another.

The sprayed fiber reinforced polymer repair system proved to be very effective in increasing the energy required to fracture the specimen. The load required for fracture of the repaired specimen was double that of the uncracked specimen. This increased load shows that the bond between the application face and the polymer was sufficient to transfer the loads in the specimen to the repair system. The failure of the polymer material, seen in the large drop in load just after cracking, could be a concern for catastrophic failure without warning signs. However, Lee and Hausmann (2003) and Lee et al. (2003) demonstrated that if the SFRP specimen is allowed to continue to ultimate failure it will absorb a considerable amount of additional energy. This additional energy is a result of the fiber reinforcing bridging the crack and regaining much of the lost load. While this accents the ductility of the SFRP repair system, the large load loss is still a cause for concern. In structures with large dead loads, a crack induced by a live or impact loading could generate enough momentum to essentially snap the fiber reinforcing before the loads are properly redistributed to them.

The fiber reinforced mortar repair system bonded sufficiently with the specimen to transfer all of the loads to the repair system. The repair system modestly increased the tensile capacity of the specimen, averaging 16% higher loads than the uncracked specimen. The mortar failed relatively quickly, however there was no sudden drop in stress when the repair system cracked. The crack propagated slowly across the face, down the sides, and then opened. The fiber reinforcement held the loads constant while the crack grew. This feature of the fiber reinforced mortar would not allow for a catastrophic failure without warning, as the opening crack and increasing deflections would be a visible warning sign.

While neither of these repair systems would stop intrusion into the specimen of water or other corrosive materials (Figure 12), they do increase the tensile strength of the cracked specimen. Restoring the original strength of the specimen is the first step in repairing the specimen, but for the repair system to be truly effective, it must do more. While the FRM specimens did exceed the original strength of the uncracked specimen, they did so utilizing

the plastic deformation region of the FRM. As was noted in the test results, the mortar had cracked but loading was continued because slope of the load to displacement curve had not changed. The testing was stopped at what could be considered the ultimate load before complete failure. For the repair system to be considered effective, the repair material should not use plastic deformation to achieve the design loads. In contrast, the loading for the SFRP specimens was stopped after the initial crack formed. The failure energy of the SFRP specimen at ultimate from Lee and Hausmann (2003) is 75% higher than the FRM specimen. This accents the greater ductility of the SFRP, while also highlighting its effectiveness as a repair system.

The combination of high initial crack strength, extreme ductility, and increased coverage illustrate that SFRP is a viable alternative for use as a repair system for concrete. The ease of application and quick curing time also enhance its viability. More testing is still required to see how SFRP performs under more realistic situations, such as application to overhead or vertical surfaces, as well as the durability of SFRP under environmental conditions such as rain, snow, or prolonged exposure to sunlight. Other comparisons to more conventional repair methods, such as epoxy injection, would also be useful to establish a better understanding of the characteristics of SFRP.

Acknowledgments

The authors gratefully acknowledge the support from Warren Environmental Inc., South Carver, MA, for providing the epoxy system, fibers and spraying equipment used in these tests. This research was supported by start-up funds provided to Dr. Lee and Summer Support Award from the University of Miami.

References

1. FU, X. AND CHUNG, D.D.L., "Effect of Curing Age on the Self-Monitoring Behavior of Carbon Fiber Reinforced Mortar," *Cement and Concrete Research*, Vol. 27, pp.1313-1318, 1997.
2. GLINICKI, M.A., "Toughness of Fiber Reinforced Mortar at High Tensile Loading Rates," *ACI Materials Journal*, Vol. 91, pp. 161-166, 1994.
3. ISSA, M.A. AND SHAFIQ, A.B., "Fatigue Characteristics of Aligned Fiber Reinforced Mortar," *ASCE Journal of Engineering Mechanics*, Vol. 125, pp. 156-164, 1999.
4. LEE, H.K. AND HAUSMANN, L.R., "Structural Repair and Strengthening of Damaged RC Beams with Sprayed FRP," *Composite Structures*, submitted, 2003.
5. LEE, H.K., SUARIS, W., AND HAUSMANN, L.R., "Experimental Study on Structural Enhancement of Sprayed Fiber-Reinforced Composites for Retrofit/Strengthening of Concrete Beams", *Composites Part B: Engineering*, submitted, 2003.
6. SOROUSHAN, P., AOUADI, F., AND NAGI, M., "Latex-Modified Carbon Fiber Reinforced Mortar," *ACI Materials Journal*, Vol. 88, pp. 11-18, 1991.
7. TANG, B., "Fiber Reinforced Polymer Composites Applications in USA," First Korea/U.S.A. Road Workshop Proceedings, Jan 28-29, 1997.
8. TANG, B. AND PODOLNY, W., "A Successful Beginning for Fiber Reinforced Polymer (FRP) Composite Materials in Bridge Applications," FHWA Proceedings, International Conference on Corrosion and Rehabilitation of Reinforced Concrete Structures, Orlando, FL, Dec 7-11, 1998.
9. WANG, Y., LI, V.C., AND BACKER, S., "Tensile Properties of Synthetic Fiber Reinforced Mortar," *Cement and Concrete Composites*, Vol. 12, pp. 29-40, 1990.
10. ZHU, M. AND CHUNG, D.D.L., "Improving Brick-to-Mortar Bond Strength By the Addition of Carbon Fibers to the Mortar," *Cement and Concrete Research*, Vol. 27, pp. 1829-1839, 1997.
11. A LOOK AT THE WORLD'S FRP COMPOSITES BRIDGES, A Publication of the Market Development Alliance, SPI Composites Institute, New York, 1998.

-
12. STANDARD TEST METHOD FOR DETERMINING FRACTURE PROPERTIES OF CONCRETE,
ACI 446, Draft 10, American Concrete Institute, Sep 26 2001.

List of Tables

Table 1. Summary of test results for specimens repaired with SFRP

Table 2. Summary of test results for specimens repaired with FRM

List of Figures

Figure 1. Application of SFRP.

Figure 2. Premixed cement containing the fibers.

Figure 3. Estimation of volume fraction of fibers using sieve analysis.

Figure 4. Application of the wet mortar on specimens.

Figure 5. Measurement of thickness of the mortar coating.

Figure 6. Support blocks: (a) Loading base with rod (left); (b) Loading base with ball (right).

Figure 7. The instrumented yoke.

Figure 8. MTS testing machine with the instrumented yoke and LVDT.

Figure 9. The load-displacement curves of the specimens repaired with SFRP.

Figure 10. The load-displacement curves of the specimens repaired with FRM.

Figure 11. The comparison of load-displacement curves between specimens repaired with SFRP and FRM.

Figure 12. Repaired Specimens: (a) SFRP; (b) FRM (Note that the repair system is only applied to the tension face, allowing for intrusion of corrosive materials from the side faces.).

Table 1. Summary of test results for specimens repaired with SFRP

Specimen	Maximum Load (N)		Percent of Repair/Precrack	Energy (J)
	Precrack	Repaired		
Polymer01	8761.94	16820.66	192%	11.13
Polymer02	8761.94	15798.12	180%	19.49
Polymer03	8761.94	12847.67	147%	3.02
Polymer04	8761.94	19064.71	218%	15.21
Polymer05	8761.94	22559.36	257%	19.93
Average	8761.94	17418.10	199%	13.76

Table 2. Summary of test results for specimens repaired with FRM

Specimen	Maximum Load (N)		Percent of Repair/Precrack	Energy (J)
	Precrack	Repaired		
Mortar01	10537.80	7525.98	71%	5.50
Mortar02	8767.52	11117.79	127%	17.40
Mortar03	8767.52	11769.16	134%	4.52
Mortar04	12205.41	14446.70	118%	14.23
Mortar05	8705.61	11792.65	135%	6.04
Average	9796.77	11330.46	116%	9.54



(a) Epoxy resin base coat



(b) Fiber application



(c) Epoxy resin top coat

Figure 1. Application of SFRP.

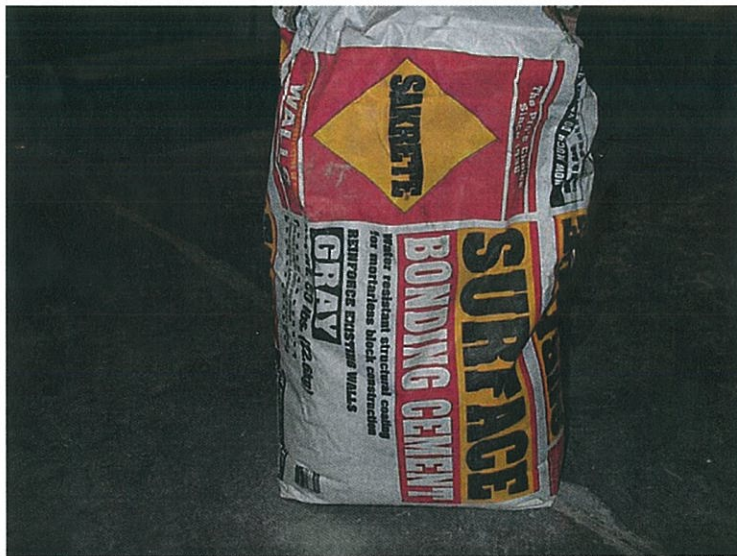


Figure 2. Premixed cement containing the fibers.

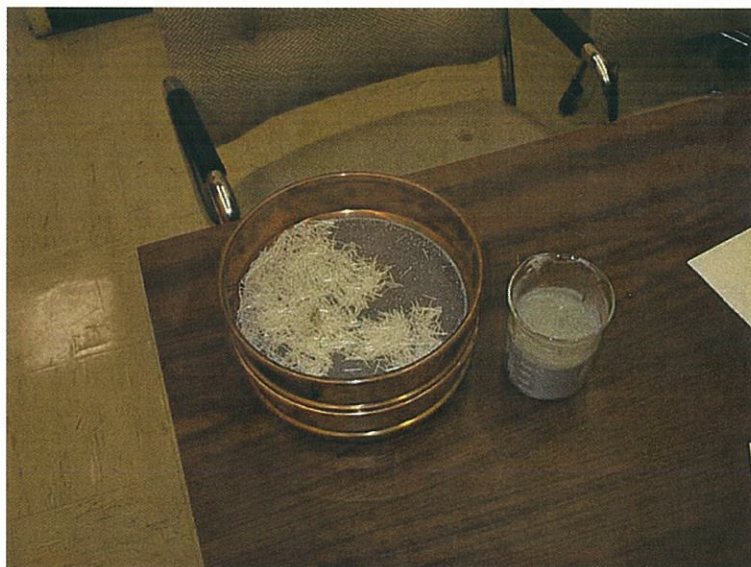


Figure 3. Estimation of volume fraction of fibers using sieve analysis.

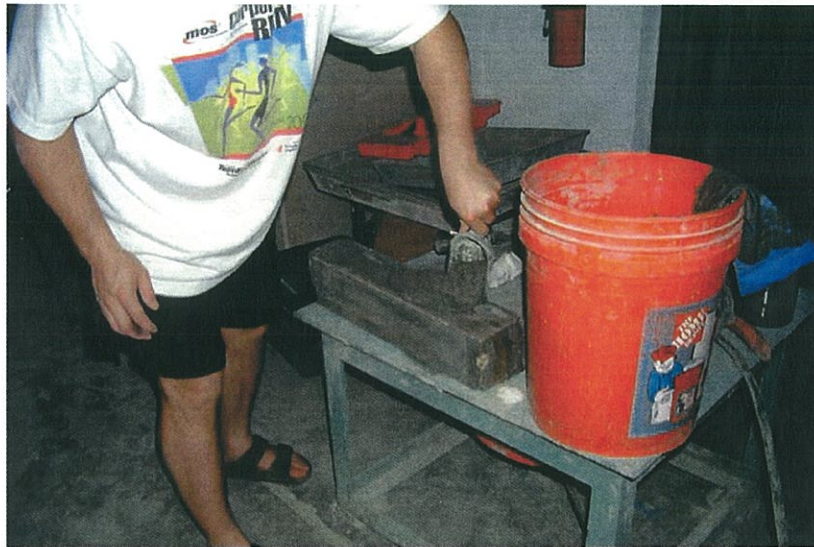
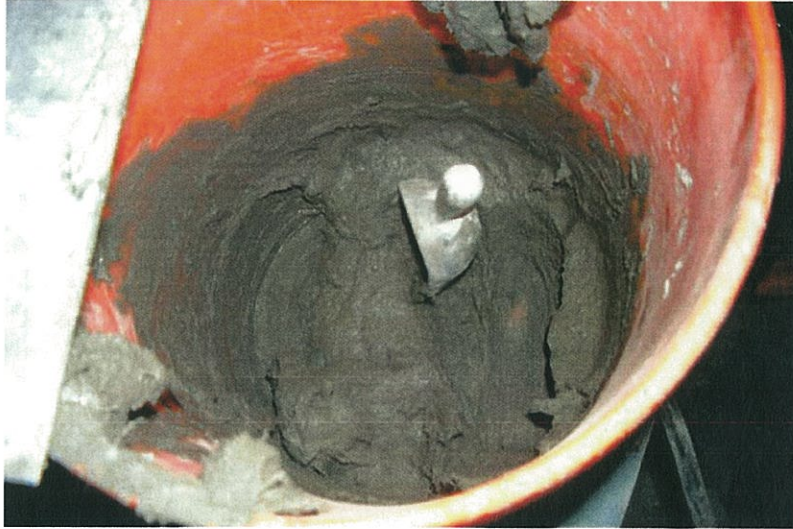


Figure 4. Application of the wet mortar on specimens.

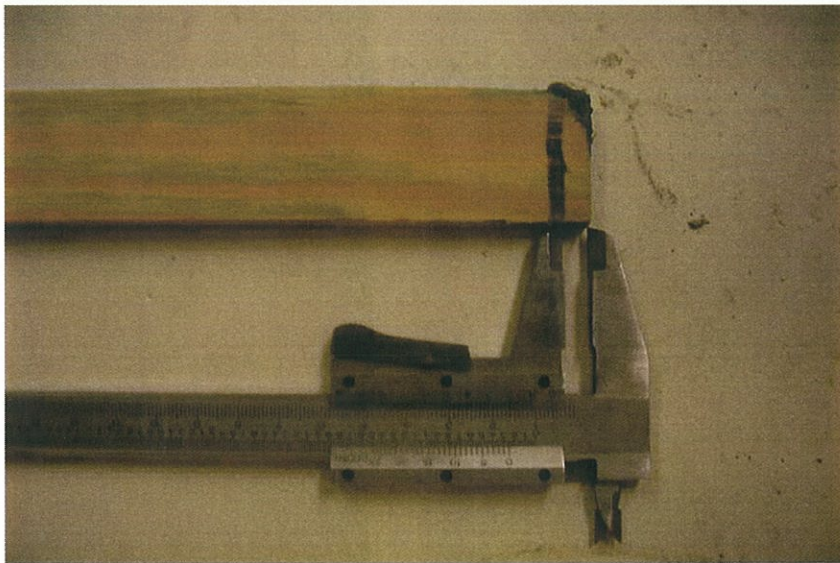


Figure 5. Measurement of thickness of the mortar coating.

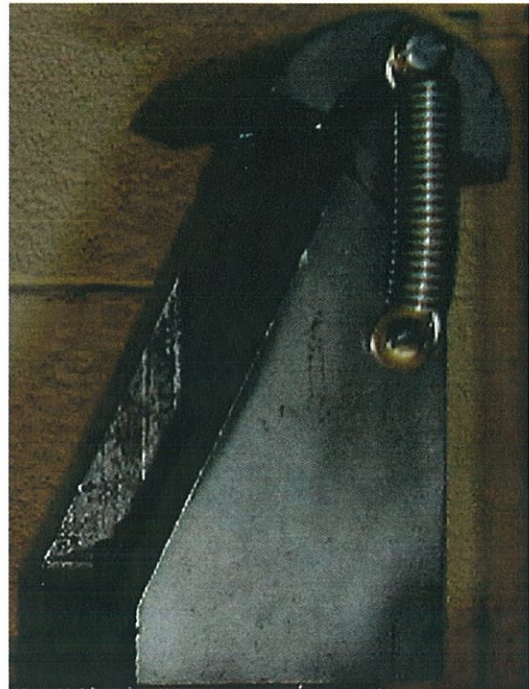


Figure 6. Support blocks: (a) Loading base with rod (left); (b) Loading base with ball (right).

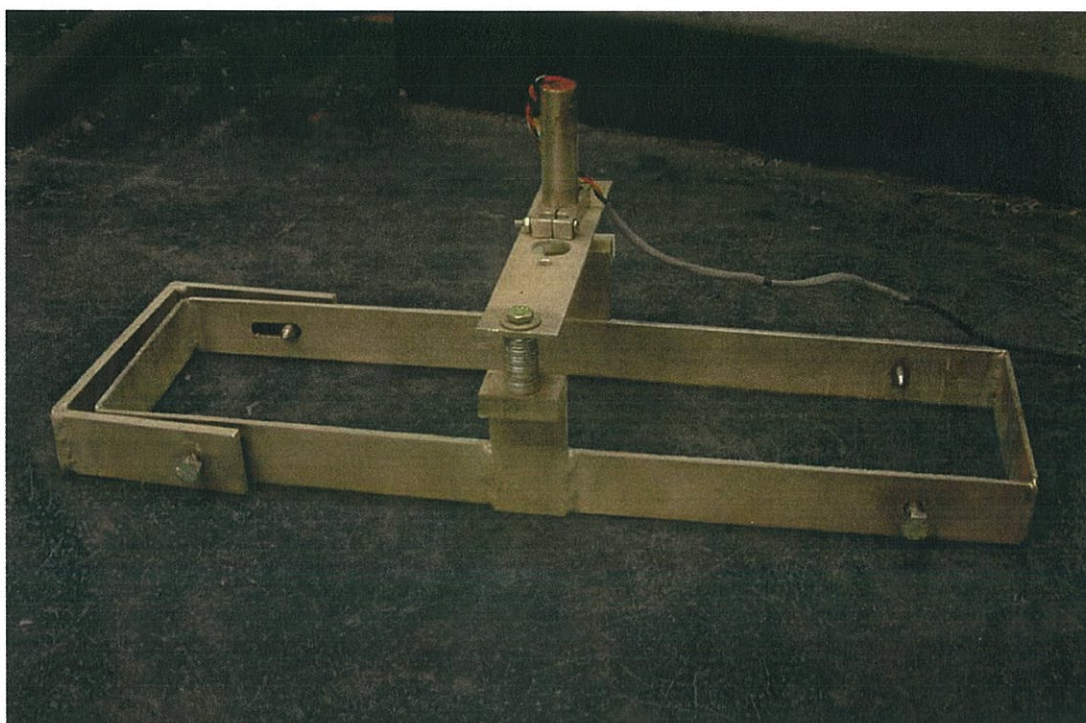


Figure 7. The instrumented yoke.

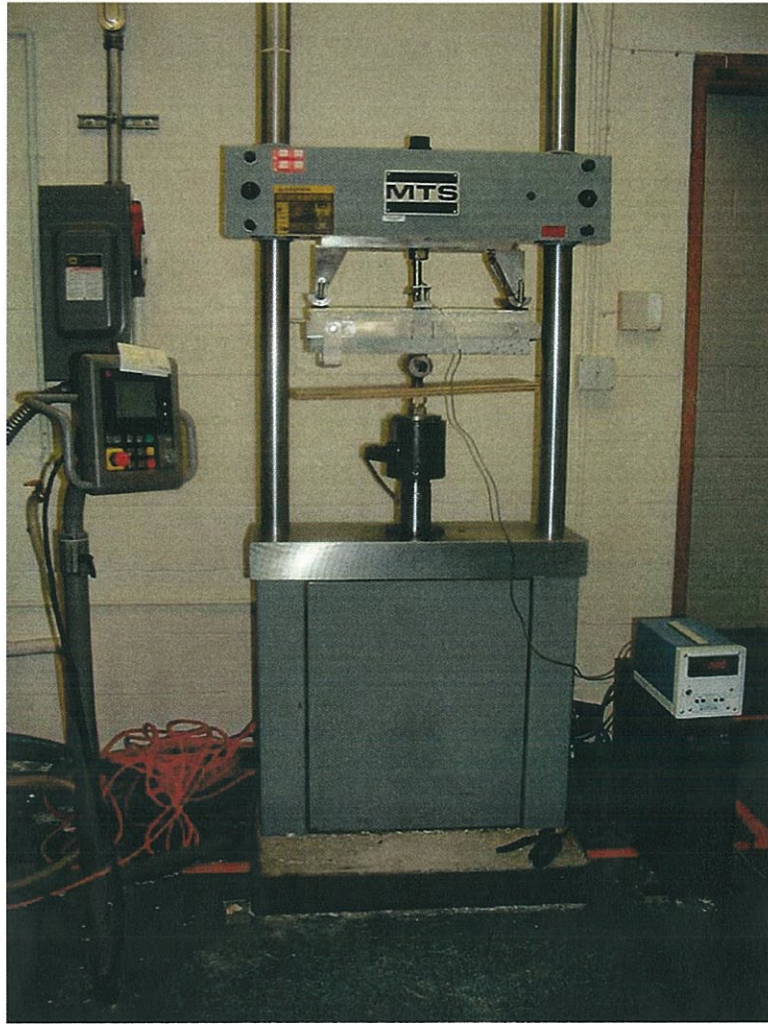


Figure 8. MTS testing machine with the instrumented yoke and LVDT.

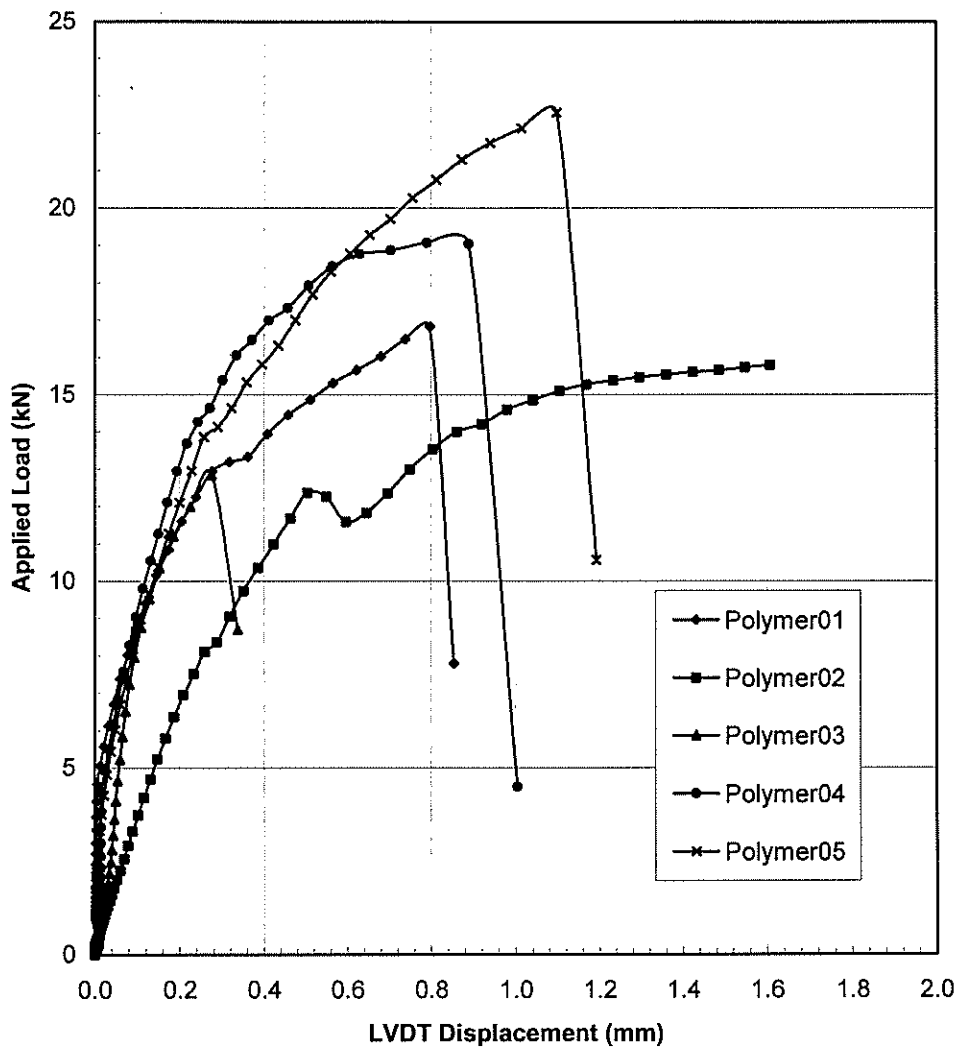


Figure 9. The load-displacement curves of the specimens repaired with SFRP.

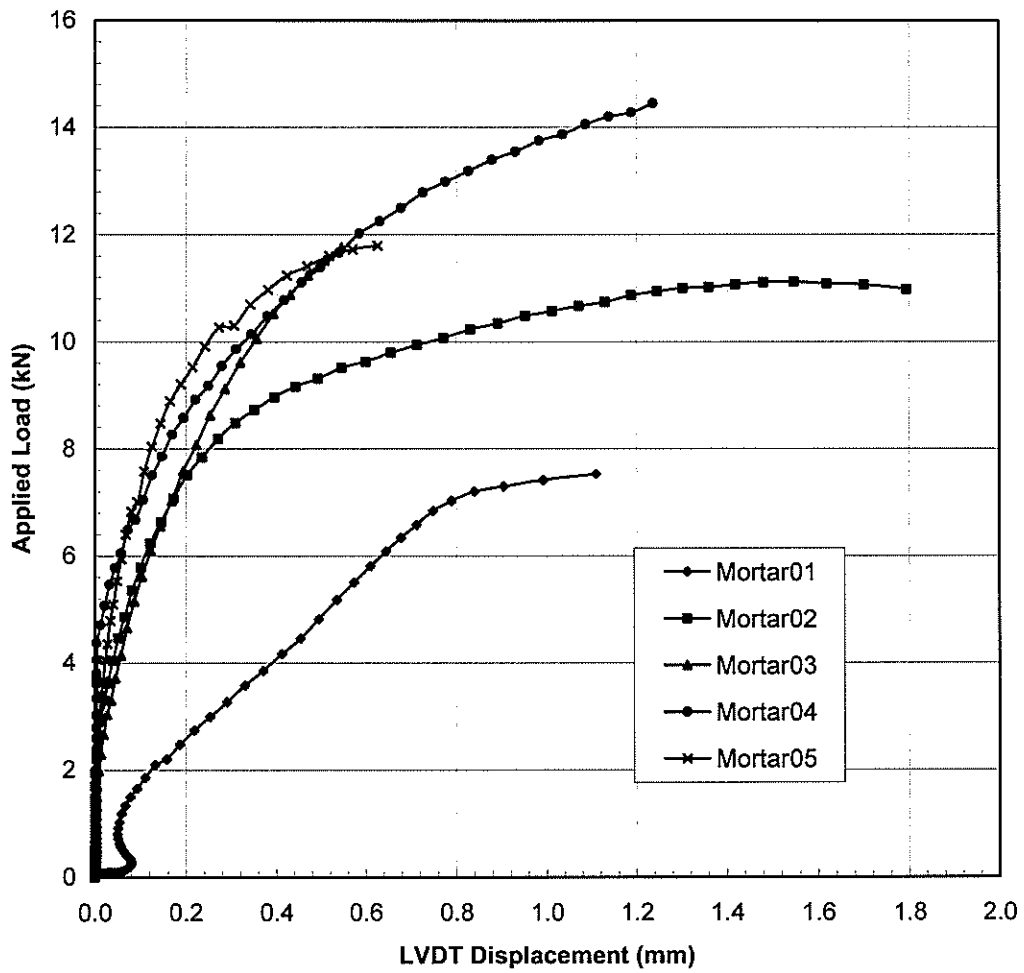


Figure 10. The load-displacement curves of the specimens repaired with FRM.

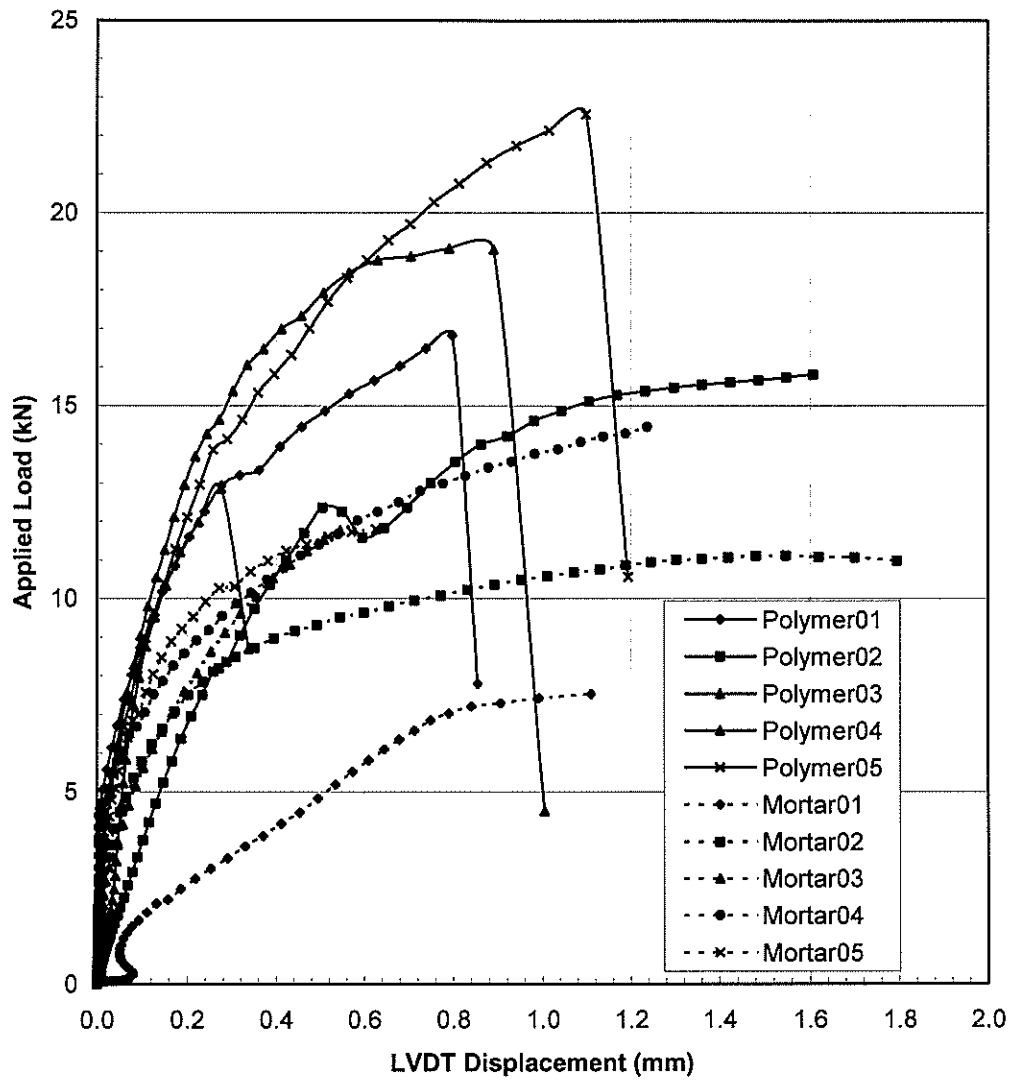
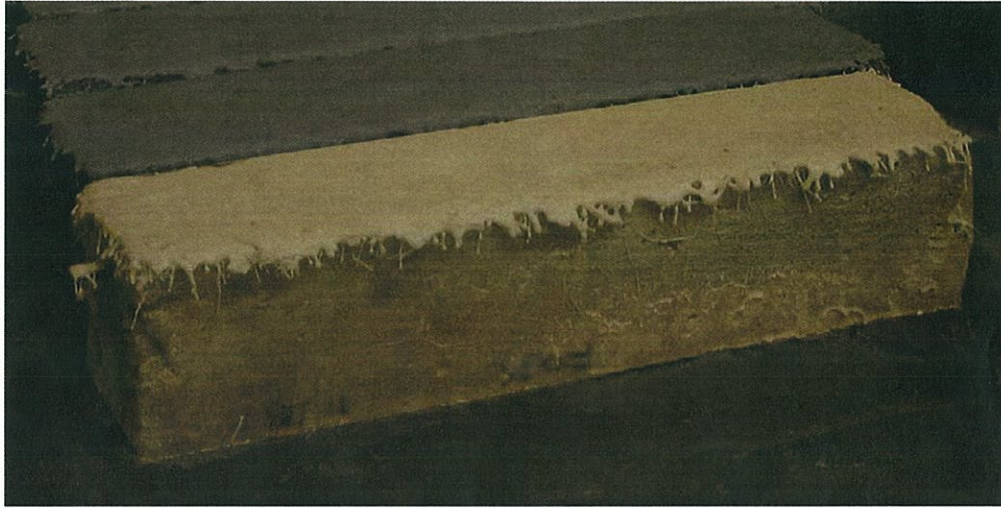


Figure 11. The comparison of load-displacement curves between specimens repaired with SFRP and FRM.



(a) SFRP



(b) FRM

Figure 12. Repaired Specimens: (a) SFRP; (b) FRM (Note that the repair system is only applied to the tension face, allowing for intrusion of corrosive materials from the side faces.).